Maintenance of photosynthetic capacity in flooded tomato plants with reduced ethylene sensitivity

Leandro Federico De Pedro[a, †], Francesco Mignolli[b,c,†,*], Andrea Scartazza[d], Juan Pablo Melana Colavita[e], Carlos Alberto Bouzo[f] and María Laura Vidoz[b,c,*]

[a]Facultad de la Producción y del Medio Ambiente, Universidad Nacional de Formosa, Ruta Nac. 86, Km 1352, CP 3613, Formosa, Argentina

[b]Instituto de Botánica del Nordeste (UNNE-CONICET), 2131 Sargento Cabral, CP 3400, Corrientes, Argentina

[c]Facultad de Ciencias Agrarias, Universidad Nacional del Nordeste, 2131 Sargento Cabral, CP 3400, Corrientes, Argentina

[d]Institute of Research on Terrestrial Ecosystems, National Research Council, 1 via Moruzzi, 56124, Pisa, Italy

[e]Instituto de Química Básica y Aplicada del Nordeste Argentino (IQUIBA, NEA-CONICET), 5470 Avenida Libertad, CP 3400, Corrientes, Argentina

[f]Laboratorio de Investigaciones en Fisiología y Biología Molecular Vegetal (LIFiBVe), ICi Agro-Litoral (UNL-CONICET), 2805 Kreder, CP 3080, Santa Fe, Argentina

Correspondence

[*]Corresponding authors,

e-mail: fmignolli80@gmail.com; malauravidoz@gmail.com

This article has been accepted for publication and undergone full peer review but has not been through the copyediting, typesetting, pagination and proofreading process which may lead to differences between this version and the Version of Record. Please cite this article as doi: 10.1111/ppl.13141

†These authors contributed equally to this work

Ethylene is considered one of the most important plant hormones orchestrating plant responses to flooding stress. However, ethylene may induce deleterious effects on plants, especially when produced at high rates in response to stress. In this paper, we explored the effect of attenuated ethylene sensitivity in the *Never ripe* (*Nr*) mutant on leaf photosynthetic capacity of flooded tomato plants. We found out that reduced ethylene perception in *Nr* plants was associated with a more efficient photochemical and non-photochemical radiative energy dissipation capability, in response to flooding. The data correlated with retention of chlorophyll and carotenoids content in flooded *Nr* leaves. Moreover, leaf area and specific leaf area were higher in *Nr*, indicating that ethylene would exert a negative role in leaf growth and expansion under flooded conditions. Although stomatal conductance was hampered in flooded *Nr* plants, carboxylation activity was not affected by flooding in the mutant, suggesting that ethylene is responsible for inducing non-stomatal limitations to photosynthetic CO_2 uptake. Upregulation of several cysteine protease genes and high protease activity led to Rubisco protein loss in response to ethylene under flooding. Reduction of Rubisco content would, at least in part, account for the reduction of its carboxylation efficiency in response to ethylene in flooded plants. Therefore, besides its role as a trigger of many adaptive responses, perception of ethylene entails limitations in light and dark

photosynthetic reactions by speeding up senescence process that leads to a progressive disassembly of the photosynthetic machinery in leaves of flooded tomato plants.

Abbreviations – *A*, net CO_2 assimilation rate; C_i, intercellular CO_2 concentration; *E*, transpiration rate;

F_v/F_m, potential efficiency of PSII photochemistry; g_s, stomatal conductance; NPQ, non-photochemical quenching; PPFD, photosynthetic photon flux density, V_{Cmax}, maximum rate of Rubisco-mediated carboxylation; WUEi, intrinsic water use efficiency; Φ_{PSII}, actual photon yield of PSII photochemistry.

Introduction

One of the most evident effects of climate change is the increase in torrential rains of short duration, resulting in an uneven distribution of precipitation along the year (Kundzewicz et al. 2007). As the intensity of rainfall and evaporation increases due to global warming, many arid areas become even more arid, while many wetlands (mainly rural areas) are subjected to more frequent floods (Voesenek and Sasidharan 2013). It has been estimated that, annually, more than 17 million km^2 are exposed to flooding (Voesenek and Sasidharan 2013) which is especially concerning for plant crop productivity in tropical and sub-tropical regions (Ashraf 2012, Pedersen et al. 2017).

Flooded soils are subjected to oxygen shortage, reduced availability of certain nutrients, lower redox potential and increased solubility of toxic ions (Horchani et al. 2008, Striker 2012). In particular, the oxygen limitation in flooded environments is caused by

a decrease in gas diffusion in water of around 10^4 times (Bailey-Serres et al. 2012), which rapidly generates a hypoxic environment in roots proximity (Ashraf, 2012).

Although little is known about the causes of photosynthesis decline in flooded plants, most plants undergo a drop in carbon assimilation rate when exposed to such stress (Yordanova and Popova 2007, Herrera et al. 2008, Bhatt et al. 2015; Mutava et al. 2015, Najeeb et al. 2015). It is believed that stomatal closure, decrease of mesophyll CO_2 conductance, chlorophyll loss, reduction of carboxylation activity and oxidative damage of photosystem II (PSII) reaction centres impair CO_2 uptake capacity in flooded plants (Ashraf 2012, Striker 2012, Pompeiano et al. 2019). In general, while a stomatal limitation could account for the initial reduction in carbon assimilation, a non-stomatal limitation takes place after longer periods from the onset of flooding stress due to the alteration of some biochemical reactions involved in photosynthesis (Chen et al. 2015, Yordanova et al. 2005). In tomato, the reduction of stomatal conductance occurs within a few hours from the onset of flooding stress (Bradford 1983). The emergence of adventitious roots with improved internal aeration partially restores stomatal opening, indicating that the loss of root function is responsible for stomatal closure and photosynthesis impairment during flooding (Else et al. 2009). Non-stomatal limitations are often related to decreases in Rubisco activity and/or its abundance (Pezeshki 2001, Ahsan et al. 2007). It has been proposed that the degradation of Rubisco and Rubisco activase due to a high proteolytic activity or ROS-mediated oxidative process is responsible for the reduction in carbon assimilation of flooded tomato plants (Ahsan et al. 2007). In some species, the decrease in leaf gas exchange parameters during flooding

could induce photoinhibition (Herrera 2013), since the limited availability of CO_2 for photosynthesis may affect the photochemical efficiency of PSII (Else et al. 2009). The reduction of maximum quantum efficiency of PSII (F_v/F_m) and the actual quantum yield of PSII (Φ_{PSII}) photochemistry during flooding, as previously observed in several species (Arbona et al. 2009, Herrera, 2013, Pompeiano et al. 2019), may indicate a damage of PSII reaction centres and limitations in the electron transport chain (Kläring and Zude 2009).

The gaseous hormone ethylene is involved in many physiological processes of a plant, such as seed germination, floral initiation, leaf senescence and organ abscission (Abeles et al. 2012). When stressed, plants generally increase ethylene biosynthesis by the induction of ACC synthase (ACS) and ACC oxidase (ACO) genes (Morgan and Drew 1997). In flooded tomato plants, ethylene production occurs according to the well-known model described by Jackson (2002), in which the ACC produced in roots is transported to the aerial part of the plant through the xylem. Once in leaves, the presence of a normal oxygen concentration allows the conversion of ACC to ethylene through the action of ACOs. The role of ethylene as a chemical trigger for adaptive strategies to cope with flooding stress has been extensively demonstrated (reviewed in Sasidharan and Voesenek, 2015). Boosted ethylene biosynthesis, followed by ethylene entrapment by water in proximity to submerged tissues, is able to induce important anatomical and biochemical changes in submerged organs. Ethylene-mediated plant adaptations to flooded environments include: aerenchyma formation as seen in maize, rice and tomato (Yamauchi et al. 2016, Mignolli et al. 2020); adventitious roots

formation as observed in species like *Solanum dulcamara* and tomato (Vidoz et al. 2010, Dawood et al. 2016); petiole hyponasty thoroughly studied in *Rumex* and Arabidopsis (van Veen et al. 2013); and internode elongation noted in deep-water rice cultivars (Hattori et al. 2009). In addition, ethylene seems to be a necessary determinant of alcohol dehydrogenase induction and the initiation of the fermentative pathway in hypoxic organs (Peng et al. 2001).

However, in spite of these beneficial responses during flooding acclimation, ethylene has some negative effects on flooding tolerance especially when produced in large amounts (Fukao et al. 2006). Indeed, injuries caused by flooding in sunflower seem to be strictly correlated to high levels of ethylene (Kawase 1974), while tolerance to partial submersion observed in the tomato mutant *aerial roots* would be associated with a lower sensitivity to the hormone (Vidoz et al. 2016). Recent experiments have shown that ethylene is responsible for lower nitrogen uptake, decreased photosynthetic activity and higher rate of fruit abscission in waterlogged cotton plants (Najeeb et al. 2015). Similarly, in tomato, flower and fruit abortion could be linked to flooding-induced ethylene synthesis (Horchani et al. 2008). This dualistic role of ethylene could be explained with a biphasic model in which plant growth is promoted or inhibited by low or high concentrations of ethylene, respectively (Pierik et al. 2006, Wi et al. 2010). According to this model, the dualistic effect of ethylene would rely upon two temporally spaced peaks of ethylene produced during stress. It is suggested that a small early ethylene emission in plants would trigger adaptive responses, whereas a second

more conspicuous ethylene peak would initiate inhibitory processes such as senescence, chlorosis and abscission (Stearns and Glick 2003).

The role of ethylene in controlling photosynthesis is still controversial and elusive. A distinction should be made between basal and stress-induced ethylene production and their respective effects on photosynthesis. Although several reports stated that a certain level of ethylene in non-stressed plants is essential for stomatal conductance and Rubisco activity (Tholen et al. 2004), it is also true that under stressful conditions ethylene build-up can be detrimental for these processes (Pierik et al. 2006). Yet, the effect of ethylene on photosynthesis in plants under stress is far from being universal because it depends on species, type of stress, leaf age and amount of ethylene produced (Khan et al. 2008, Djanaguiraman et al. 2011, Masood et al. 2012, Ceusters and Van de Poel 2018). In our work, we investigated the effects of attenuated ethylene perception on photosynthesis capacity in tomato plants exposed to flooding. To this purpose, the tomato mutant *Never ripe* (*Nr*), which is characterized by a defective ethylene receptor (LeETR3, Lanahan et al. 1994), offers a valid help to understand the role of ethylene signalling in biotic and abiotic stress tolerance (Ciardi et al. 2000, Gratão et al. 2009, Monteiro et al. 2011, Poór et al. 2015). We indirectly assessed the impact that flooding-induced ethylene has on plants ability to photosynthesize, shedding light on what could be considered the dark side of ethylene-mediated responses to abiotic stresses. Considering the increased frequency of flooding events in agricultural areas of the world, we believe that our work could provide a base for more applied studies focused on managing detrimental ethylene levels in flooded crops.

Materials and methods

Plant growth conditions and experiment set-up

Tomato (*Solanum lycopersicum* L.) seeds of Pearson (PRS, accession LA0012) and the spontaneous isogenic mutant *Nr* (accession LA0162) were obtained from The Tomato Genetics Resource Center (University of Davis, CA, USA). After 7 days from sowing, seedlings were transplanted in 250 cm^3 plastic containers in commercial peat-based substrate (Dynamics 2, Agri Service, Buenos Aires, Argentina). Seedlings were kept in a controlled growth chamber at 26 ± 2°C and 60% relative humidity (RH), illuminated by high-pressure sodium lamps with a cycle of 15/9 h, light/dark and an irradiance of 500 μmol m^{-2} s^{-1}. Plants were watered with ¼ Hoagland solution periodically, in order to maintain the soil at field capacity.

When plants were 28 days old, they were placed in transparent plastic containers of approximately 30 l (390 × 280 × 280 mm). The flooding treatment, more specifically a partial submersion (Sasidharan et al. 2017), was performed by adding tap water to these containers up to 15 mm above the cotyledonary nodes. In order to prevent pot buoyancy and ensure that plants remained partially submerged, gravel was scattered on top of the soil (Fig. S4A). Pots of control plants were placed in the same containers but the substrate was maintained at field capacity for the duration of the experiment by watering regularly. In order to maintain all plants with the same light intensity, the position of containers was changed every day. Plants were maintained under flooding conditions for six days.

Leaf samples (20 to 100 mg of fresh weight) from control and flooded PRS and *Nr* plants used for pigment analysis, total soluble proteins, proteases activity, and Rubisco protein quantification were collected with a cork borer from the 3rd fully expanded leaf (terminal leaflet plus lateral leaflets, Fig. S4B). Each sample consisted of a pool of at least three leaves from three different plants. Samples were collected at the sixth day from the beginning of experiments and immediately stored at -70°C up to analysis.

Growth parameters and leaf pigment analysis

In order to measure leaf area, leaves of plants at day 6 from the beginning of the experiment were removed and photographed on a flat surface. Digital photos were taken and analysed with the picture processing software ImageJ (National Institutes of Health, http://rsb.info.nih.gov/ij) to quantify leaf area. Plant biomass was obtained by weighing oven-dried (70°C) leaves, stems and roots (seminal plus adventitious roots). Specific Leaf Area (SLA) was calculated by dividing leaf area by its dry weight. Leaf, Stem and Root Mass Fraction (LMF, SMF and RMF, respectively) were calculated by dividing leaf, stem and root dry weight by total plant biomass. Leaf chlorophyll content was estimated with a portable chlorophyll meter device SPAD-502 (Konica Minolta, Osaka, Japan). Quantification of chlorophyll *a* (Chl *a*), chlorophyll *b* (Chl *b*), and total carotenoids (Car) was performed according to Caser et al. (2016). Leaf pigment content was calculated according to Lichtenthaler (1987).

Leaf gas exchange and fluorescence analyses

Leaf gas exchange in control and submerged PRS and *Nr* plants was carried out with a LI-6400XT portable system (Li-Cor Inc., USA) equipped with 6400-02B LED light source chamber. Measurements were made on the terminal leaflet of the 3rd fully expanded leaves (Fig S4B) between 9:00 am and 12:00 pm. The instrument was set at 500 μmol m^{-2} s^{-1} of photosynthetic photon flux density (PPFD; 10% blue and 90% red light), foliar temperature of 25 ± 1°C, 60% RH, CO_2 concentration of 400 ppm and 500 mmol s^{-1} of flow rate. Instantaneous measurements of net CO_2 assimilation rate (A), stomatal conductance (g_s), transpiration rate (E) and intercellular CO_2 concentration (C_i) were recorded at steady state (~3 min).

In order to estimate Rubisco activity, an A/C_i curve was performed exposing the leaf to a range of distinct ambient CO_2 concentrations (C_a, in the LI-6400 chamber) between 50 and 400 μmol mol^{-1} (~10 min for each data point) under saturating light conditions (1500 μmol m^{-2} s^{-1} PPDF), according to the method described by Centritto et al. (2003). The maximum rate of Rubisco-mediated carboxylation (V_{cmax}) was estimated by fitting the CO_2-limited portion of the photosynthetic CO_2 response curve (C_i lower than 200 μmol m^{-2} s^{-1}) to the biochemical model in Farquhar et al. (1980), as described by Scartazza et al. (2016). To avoid errors due to CO_2 leakage, a relatively high flow rate was maintained inside the chamber (700 mmol s^{-1}) and the absence of significant leakage effects was verified according to Flexas et al. (2007). When necessary, measurements were corrected to 25 °C using the temperature responses of Bernacchi et al. (2001) for the Rubisco-limited portions of the A/C_i curves.

Chlorophyll fluorescence parameters were measured using a Mini-PAM fluorimeter (Heinz Walz, Effeltrich, Germany) and the fluorescence terminology used by Scartazza et al. (2016) was adopted. Measurements were performed on the terminal leaflet of the 3rd leaf of each plant (Fig. S4B). Instantaneous measurements were performed at 2, 4 and 6 days after the start of the flooding treatment, between 09:00 and 11:00 am, at growth chamber light conditions (500 μmol m^{-2} s^{-1}). Φ_{PSII} was determined as $\Phi_{PSII} = (F_m'-F')/F_m'$ at steady state. F_m' is the maximum fluorescence of dark-adapted leaves after a flash of saturating light. F' is the fluorescence at the actual state of PSII reaction centres during actinic illumination. F_v/F_m was calculated on dark-adapted leaves (at least 30 min of leaf acclimation to darkness) as $F_v/F_m = (F_m-F_o)/F_m$, where F_m is the maximum fluorescence yield in the dark and F_0 is the minimal fluorescence emitted by dark-adapted leaves. The non-Photochemical Quenching (NPQ) was calculated according to the Stern–Volmer equation as $NPQ = (F_m/F_m')-1$.

Total soluble protein content and total protease activity

Leaf total soluble proteins were extracted from about 20 mg of frozen leaf samples. Homogenization of leaf tissues was performed in ice-cold extraction buffer 50 mM Tris-HCl pH 7.4, 1 mM EDTA, 1 mM DTT, Triton X-100, 0.1% (v/v). After centrifugation at 12 000 *g* for 10 min at 4°C, the supernatant was recovered and total soluble proteins were quantified by measuring the absorbance at 595 nm with Bradford reagent ("Bio-Rad Protein Assay" kit, Bio-Rad, USA).

Total protease activity was performed by following the method described by Battelli et al. (2011). Leaf protein extracts obtained by homogenizing leaf samples in ice-cold buffer [50 mM Tris-HCl pH 7.0, 10 mM 2-mercaptoethanol, 2.5% insoluble polyvinylpolypyrrolidone (PVPP) and 0.1% Triton X] were assayed. The pH of the reaction mixture was adjusted to 5.5 since proteolytic activity showed its maximum at this pH (data not shown). The reaction mixture consisted of 225 µl of 50 mM acetate buffer pH 5.5, 250 µl of 0.4% azocasein (w/v, diluted in 0.1 N NaOH), 5 µl of 0.25 M 2-mercaptoethanol and 20 µl of leaf protein extract. After incubation for 10 h at 32°C the reaction was stopped by the addition of 50% (w/v) trichloroacetic acid (TCA) followed by centrifugation at 4°C for 10 min at 14 000 *g*. For each extract, a blank was obtained by adding 50% TCA to the reaction mixture prior to the incubation in order to prevent any proteolytic activity. Change of absorbance of "azo" dye between samples and blanks was measured spectrophotometrically at 440 nm. The protease activity was expressed as ΔABS μg^{-1} of proteins min^{-1}.

Quantification of Rubisco large subunit

Quantification of Rubisco large subunit was performed according to Westbeek et al. (1999) with some modifications. Leaf proteins were obtained according to the previously described method. Twenty-five µg of proteins were diluted in 1 M Tris HCl pH 6.8, 10% SDS, glycerol, 2-mercaptoethanol and bromophenol blue. Each preparation was heated at 95°C for 4 min. The separating gel was prepared with 30% acrylamide:bisacrylamide (39:1 ratio), 1.5 M Tris-HCl buffer pH 8.8, distilled water,

10% SDS, 10% ammonium persulfate (APS) and tetramethylethylenediamine (TEMED). Stacking gel was prepared with 30% acrylamide:bisacrylamide (39:1 ratio), 0.5 M Tris-HCl, distilled water, 10% SDS, 10% APS and TEMED. Kaleidoscope Prestained Standards was used as molecular weight marker. The electrophoretic run was performed in glycine/Tris-HCl buffer at constant voltage and variable amperage 50 mA for 60 min and 150 mA for 90 min. Protein binding was performed by incubating the gel for 30 min in a solution of 50% methanol, 10% acetic acid and 40% distilled water. Gel staining was carried out in a solution of 50% methanol, 10% acetic acid, 40% distilled water and 0.25% Coomassie brilliant blue r-250 for 120 min. Finally, the gel was discoloured in a solution of 5% methanol, 7.5% acetic acid and 87.5% distilled water for approximately 240 min. The Rubisco large subunit (RcbL, *c*. 56kD) was quantified by measuring the band surface with the open- source software GelAnalyzer 2010 (http://www.gelanalyzer.com/index.html).

Gene expression analysis

In order to analyse the expression of tomato *MSRA*, *SlERF-A2*, *CYP-1*, *CYP-2* and *CYP-3, rbcL and rbcS* genes, we followed the protocol described by Mignolli et al. (2012). Real-Time PCRs were performed using the HOT FIREPol® reaction mixture EvaGreen® qPCR Mix Plus ROX (Solis BioDyne, Estonia). Relative expression levels were obtained using *LeEf1α* as internal reference gene. Primer sequences are listed in Supporting Information Table S1.

Statistical analyses

Statistical analyses were performed using GraphPad Prism 6.0 statistical software (www.graphpad.com).For each graph, data were analysed with D'Agostino-Pearson omnibus normality test. Whenever data fulfilled the normality requisite, one-way ANOVA and Tukey's HSD test were performed (Fig. 1A-B; Fig. 2B,F; Fig. 3A,C; Fig. 4B,D; Fig. 5A,C; Fig. 6A-B; Fig. 7A-F; Fig. S1A-D; Fig. S2A-D; Fig. S3A-F); otherwise, the non-parametric Kruskal-Wallis test was carried out (Fig. 2C-E; Fig. 3B; Fig. 4A,C; Tabel 1; Fig. S2E,F) .

Results

Ethylene responsiveness is attenuated in leaves of flooded Nr plants

In order to ascertain whether *Nr* leaves are actually less sensitive to ethylene when plants are exposed to flooding stress, we analysed the expression of two ethylene responsive genes. The *MSRA* (methionine sulfoxide reductase) gene, formerly known as *E4*, is strongly upregulated in response to ethylene during the tomato ripening process (Lincoln et al. 1987; Montgomery et al. 1993) and is also induced in vegetative parts of tomato plants when exposed to exogenous ethylene (Vidoz et al. 2016). Similarly, the *SlERF-2A* (ethylene response factor, formerly *LeERF1*) gene, which is part of the ethylene signalling system, shows a strong upregulation in ethylene-treated fully expanded tomato leaves (Tournier et al. 2003, Pirrello et al. 2012). Both *MSRA* and *SlERF-2A* were induced on the second day in the 3rd leaves of PRS flooded plants indicating an activation of ethylene signalling in those leaves. However, in leaves of *Nr*

flooded plants, *MSRA* induction levels were about half of those in PRS and *SlERF-2A* transcript abundance remained as low as in control plants (Fig. 1).

Nr retains leaf pigments in flooded plants

Reduced ethylene perception in *Nr* limited flooding-induced green pigment loss in the 3rd leaf (Fig. 2A). While in submerged PRS plants SPAD units progressively declined after the second day of stress, in submerged *Nr* plants this index was maintained practically unchanged (Fig. 2B). After 6 days of flooding, Chl *a* content significantly decreased in 3rd and 4th leaves of PRS stressed plants with respect to non-flooded plants (Figs 2C and S1A), while no significant change was observed in *Nr* plants. Regarding Chl *b* content, no variation was observed in 3rd and 4th leaves of both genotypes in response to flooding (Figs 2D and S1B). Total carotenoids (Car) content in *Nr* did not change in response to flooding while a 16 and 22% decrease was observed in 3rd and 4th leaves of PRS, respectively (Figs 2E and S1C). Carotenoids to total chlorophylls ratio, i.e. Car/Chl (*a*+*b*), did not change in 3rd and 4th leaves of flooded PRS plants while it increased in 3rd leaves of flooded *Nr* plants (Figs 2F and S1D).

***Nr* mutation limits flooding-induced leaf area reduction**

Total biomass significantly decreased in flooded PRS and *Nr* plants (Tabel 1). However, differently from PRS in which flooding stress caused an abrupt decrease in leaf area this parameter did not change in flooded *Nr* plants. Leaf Mass Fraction (LMF), which indicates the proportion of biomass allocated to leaves, was lower in both PRS

and *Nr* flooded plants respect to their controls. Regarding Stem Mass Fraction (SMF), there was an increase in PRS and *Nr* flooded plants in comparison with their controls. The decrease in Root Mass Fraction (RMF) observed under flooded conditions was similar in both genotypes, when compared to their respective controls. The Specific Leaf Area (SLA) remained unchanged in flooded PRS plants with respect to the controls but in *Nr* this parameter increased by 42% under flooding (Tabel 1).

Flooded plants of Nr exhibited higher PSII photochemical efficiency

In order to ascertain whether the difference in leaf pigment content in *Nr* reflected an alteration of the PSII photochemistry, we measured several parameters related to chlorophyll *a* fluorescence. In PRS, F_v/F_m decreased as early as the second day of flooding in 3rd (Fig. 3A) and 4th leaves (Fig. S2A), whereas it decreased only at or after 4 days in 3rd and 4th leaves of *Nr*, respectively (Figs 2A and S2A). The reduction of F_v/F_m in 3rd leaves of flooded PRS plants was always stronger than in *Nr* throughout the flooding period (Fig. 3A). The decrease of Φ_{PSII} in flooded PRS plants started as soon as the second day of treatment, whereas a reduction in *Nr* was observed only after 4 days of flooding (Figs 3B and S2B); interestingly, in both time points, levels attained by the mutant were higher than in the wild type. While no statistical difference was observed in PRS plants under flooding and control conditions regarding NPQ, this parameter increased after 4 days of flooding in the 3rd leaf of *Nr* (Fig. 3C).

***Nr* mutation induces photosynthetic non-stomatal limitations**

In control *Nr* plants, *A* was maintained at the same level as in control PRS plants, and both genotypes showed a significant reduction in this parameter when flooded (Figs 4A and S2D). Similarly, as early as the second day from the onset of flooding, plants of both genotypes underwent a drastic decrease of *g*s in 3rd and 4th leaves (Figs 4B and S2E). A reduction in *E* levels was observed after 2 and 4 days of treatment in 3rd leaves of *Nr* and PRS plants, respectively (Fig. 4C). Notably, *C*i did not significantly change in flooded PRS plants whereas it significantly decreased in 3rd and 4th leaves of flooded *Nr* plants at 2, 4 and 6 days after the beginning of the experiment (Figs 4D and S2F). Intrinsic water use efficiency (WUEi) was calculated as the ratio between *A* and g_s. The ratio was consistently higher in leaves of flooded *Nr* plants with a peak after 4 days that almost doubled the control value (Fig. 5A). On the contrary, in flooded PRS plants, WUEi was constantly kept at nearly the same level as in non-flooded plants (Fig. 5A). Variation of *A* in response to different concentrations of CO_2, produced the A/C_i curve shown in Fig. 5B. The initial slope (dA/dC_i) of the CO_2-limited portion of the A/C_i curve provides a measure of carboxylation efficiency and allows estimating the maximum carboxylation rate of Rubisco (Vc_{max}). While flooding caused a dramatic reduction of carboxylation efficiency in PRS as indicated by the reduced slope of the A/C_i curve (0.054 vs 0.024 for control and flooding, respectively), the *Nr* slope was only slightly affected (0.074 vs 0.065 for control and flooding, respectively) (Fig. 5B). Consequently, under flooding conditions, Vc_{max} in PRS was reduced to less than a half of controls (48.6 vs 23.2 μmol m^{-2} s^{-1} for control and flooding, respectively), whereas no significant differences were observed in *Nr* (Fig. 5C).

Higher Rubisco abundance in Nr flooded plants is due to lower proteolytic activity

Following, we sought to determine whether higher carboxylation activity in *Nr* was dependent on higher abundance of Rubisco enzymes. For this, we first examined the transcript levels of genes encoding the large and small Rubisco subunits (*rbcL* and *rbcS*, respectively). In both genotypes, these genes were strongly downregulated in response to flooding (Fig. 6A,B). In particular, the expression of *rbcL* and and *rbcS* declined as early as two days after flooding in both genotypes, with *rbcS* expression abruptly dropping to levels that were 7 to 50 times (PRS) and 3 to 46 times (*Nr*) lower than control plants.

Although flooding decreased the abundance of Rubisco large subunits in both genotypes, its relative content was approximately twice as high in flooded *Nr* compared to PRS (Fig. 7A). In order to test whether this difference in Rubisco protein content would rely on a reduced proteolytic activity in flooded *Nr*, we analysed total protein content, total protease activity and the expression of three cysteine protease genes (*CYP-1*, *-2* and *-3*). In both genotypes, total soluble protein content decreased in response to flooding, but in *Nr* the level was 36% higher than in PRS (Fig. 7B). In addition, total protease activity in flooded *Nr* was 26% lower than in PRS (Fig. 7C), which correlates with null (*CYP-2* and *CYP-3*) or very low (*CYP-1*) induction of cysteine protease genes in flooded mutant plants. Differently, the expression of these

genes was strongly induced in leaves of flooded PRS plants, reaching levels that were 9, 5 and 3.5 times higher than in control plants (Fig. 7D-F).

Discussion

Soil flooding is considered one of the most concerning events associated with climate change (Pedersen et al. 2017). One of the earliest responses in tomato, when exposed to such stressful conditions, is the high production of ethylene (Vidoz et al. 2010). This gaseous hormone, besides triggering important adaptive mechanisms (Sasidharan and Voesenek 2015), is believed to be detrimental for some vital metabolic processes (Gepstein and Glick 2013). Indeed, post-submergence survival of Arabidopsis plants appears to be severely challenged by the sudden increase of ethylene production that triggers an early senescence programme (Yeung et al. 2018).

In this work we sought to demonstrate, by using the *Nr* mutant, that reduced ethylene sensitivity allows plants to retain their photosynthetic capacity when subjected to partial submersion. Although, ethylene levels produced in leaves of flooded *Nr* plants are similar to those in wild type leaves (Vidoz et al. 2010), the lack of functionality of the NR/ETR3 ethylene receptor in the mutant seems to confer only partial ethylene responsiveness, as indicated by the low or no induction of two ethylene-inducible genes *MSRA* and *SlERF-2A*, respectively (Fig. 1).

While leaf pigment retention has often been associated with flooding tolerance (Fukao et al. 2006, Arbona et al. 2009, Sone et al. 2012, Mutava et al. 2015), chlorophyll loss is one of the most evident events occurring under flooding conditions in many flooding-

sensitive plants (Ella et al. 2003, Smethrust and Shabala 2003, Ezin et al. 2010). Our data show that leaves from *Nr* plants subjected to partial submersion are greener than those of wild type plants exposed to the same conditions (Fig. 2A), and this corresponds to higher chlorophyll content in *Nr* leaves (Fig. 2B). In agreement with our observations, reduced endogenous ethylene by the introduction of the bacterial ACC-deaminase gene, which reduced ACC levels in transgenic tomato plants, has been reported to restrain chlorophyll loss in flooded tomato plants (Grichko and Glick 2001). Chlorophyll loss in PRS is accompanied by a reduction in Chl *a* but not in Chl *b*, which indicates a change in the photosynthetic pigment stoichiometry during flooding (Figs 2C,D and S1A,B). Chl *a* retention in *Nr* could be considered as an index for relative higher quantity of PSII reaction centres (Mishra et al. 2008) and may indicate a more efficient photochemical energy conversion process at PSII level (Scartazza et al. 2016, Mariotti et al. 2018). Interestingly, carotenoids (Car) content did not change in *Nr* leaves of flooded plants while it significantly decreased in PRS ones (Figs 2E and S1C), indicating an effect of ethylene in flooding-induced carotenoids loss. Previous work by Chen and Gallie (2015) reported that an Arabidopsis ethylene overproducer mutant was impaired in the ability to convert violaxanthin to zeaxanthin making the plant more sensitive to reactive oxygen species and more susceptible to photoinhibition. Indeed, due to the role of these molecules as photoprotective agents, the retention of carotenoids in plants under stress may prevent ROS generation and improve excess energy dissipation as heat (Dall'Osto et al. 2005, Demmig-Adams and Adams 2006, Das and Roychoudhury 2014).

Our observations indicated that flooding stress has a big impact on chlorophyll fluorescence parameters (Fig. 3A-C) confirming the susceptibility of tomato to this stress (Else et al. 2009; Bhatt et al. 2015). As reported in tomato, reduction of F_v/F_m is a common response to flooding stress (Fig. 3A; Else et al. 2009, Ezin et al. 2010, Bhatt et al. 2015). However, higher F_v/F_m and Φ_{PSII} values were found in flooded *Nr* plants respect to PRS (Fig. 3A,B). This, in concordance with similar levels of Chl *a* between control and flooded *Nr* plants (Fig. 2C), reveals lower damage of PSII reaction centres and greater efficiency in the use of light in photochemical processes when ethylene perception is attenuated. To note, concomitantly with a general maintenance of F_v/F_m, the NPQ parameter increased after 2 days of flooding in *Nr* while no clear change was observed in PRS (Fig. 3C). The higher NPQ activity respect to controls, associated with higher carotenoids content (Figs 2E, S1C), supports the idea of a more efficient non-radiative energy dissipation pathway, a photoprotective mechanism when ethylene perception is low (Dall'Osto et al. 2005, Demmig-Adams and Adams 2006, Moles et al. 2016, Scartazza et al. 2016). Overall, these data indicate that flooding-induced ethylene leads to a reduction of PSII efficiency making flooded plants more susceptible to photoinhibition.

Flooding stress impairs root hydraulic conductivity and the ability to take up water from the soil (Bradford 1983, Horchani et al. 2008, Else et al. 2009). We show that both *Nr* and PRS respond similarly to flooding with an abrupt decrease of g_s (Figs 4B and S2E) in order to prevent water loss through transpiration (Fig. 4C). Although *A* also diminished in response to the partial stomatal closure (Figs 4A and S2D), WUEi in *Nr*

increased after the start of the flooding and was significantly higher than in PRS (Fig. 5A). As reported for waterlogging-susceptible tomato genotypes, reduction of g_s is often accompanied by increased intercellular concentration of CO_2 (C_i) suggesting that substomatal CO_2 is not efficiently consumed by the plants (Bradford 1983, Else et al. 2009, Bhatt et al. 2015). Interestingly, while high C_i values were observed in PRS, internal CO_2 concentration was always lower in *Nr* (Figs 4D and S2F). Based on our results, we believe that the reduction of *A* in *Nr*, accompanied by a strong increase of WUEi and a lowered C_i, indicates a predominant role of stomatal limitations on photosynthesis. On the contrary, a high C_i and low WUEi in PRS suggest that non-stomatal limitations play a major role in determining its lower photosynthetic CO_2 uptake capacity, possibly due to reduced enzymatic activity, low carboxylation efficiency, chlorosis and leaf senescence (Kozlowski 1984, Ashraf and Rehman 1999, Mielke and Schaffer 2010, Herrera 2013, Pompeiano et al. 2019). Moreover, carboxylation efficiency (Fig. 5B) and maximum rate of carboxylation (V_{Cmax}, Fig. 5C), clearly show that Rubisco activity was only slightly affected by the stress in *Nr*, suggesting that ethylene could limit leaf photosynthetic capability and affect the carboxylation pathway at some point. Rubisco activity is known to be correlated with the amount of Rubisco protein which, in turn, depends on the rate of its biosynthesis and degradation (Parry et al. 2008). However, Rubisco genes *rbcL* and *rbcS* were strongly downregulated in flooded plants (Fig. 6A,B). In spite of the very low expression of *rbcL* and *rbcS* genes in flooded *Nr* plants (Fig. 5A,B), these plants retained higher relative content of rbcL protein with respect to PRS (Fig. 7A). Although we cannot exclude the

effect of inhibitors on catalytic performances of Rubisco (Parry et al. 2002), we suggest that the higher abundance of Rubisco protein observed in *Nr* is the consequence of a reduced proteolytic activity (Fig. 7C).

Reduced biomass in flooded plants (Tabel 1) is very likely the result of impaired net carbon assimilation (*A*, Figs 4A and S2D). Although, the fraction of total biomass that was allocated to different organs was similar between PRS and *Nr*, leaf area was significantly reduced in flooded PRS plants whereas it remained at control levels in *Nr* (Tabel 1). In addition, higher SLA in flooded *Nr* plants (Tabel 1) may indicate better light interception and carbon assimilation per unit of leaf biomass when carbon demand is high in response to the stress (Bertin and Gary 1998, Jullien et al. 2009, Weraduwage et al. 2015). In agreement with our findings, it has been reported that plants with reduced ethylene sensitivity are characterized by a larger leaf area than their wild type when exposed to high ethylene concentrations (Tholen et al. 2004). Even though in certain species a basal level of ethylene seems to be essential under normal conditions, it exerts negative effects on photosynthesis when it transiently accumulates in response to stress or in senescing leaves (Ceusters and Van de Poel 2018). Indeed, the induction of premature senescence in response to stress is one of the deleterious effects of ethylene (Sade et al. 2018). As part of the senescence programme, the disassembly of the photosynthetic apparatus is a common feature that occurs in leaves of plants subjected to abiotic stress (Khanna-Chopra 2012). However, our data showed that chlorophyll and protein degradation were delayed in flooded *Nr* plants (Figs 2A-C and 7B) since total protease activity was lower than in PRS (Fig. 7C) and all

the analysed cysteine protease genes (*CYP-1*, *-2* and *-3*) showed little or no induction in flooded mutant plants (Fig. 7D-F). It is believed that the decline of photosynthesis below certain levels acts as one of the signals inducing leaf senescence (Quirino et al. 2000). Under flooding conditions, both PRS and *Nr* underwent a decrease of CO_2 assimilation (Figs 4A and S2D) and a strong downregulation of some photosynthesis genes (*rbcL*, *rbcS*, Fig. 5A,B and *CAB5*, data not shown), suggesting that this decrease was triggered by a stress factor and not by the ability of the plant to perceive ethylene. However, the expression of some senescence-associated genes such as *CYP-1*, *CYP-2* and *CYP-3* (Drake et al. 1996) was suppressed in flooded *Nr* (Fig. 7D-F). Taken together, our experiments have revealed some aspects of ethylene insensitive plants that could prove beneficial when they are exposed to flooding stress for few days. Indeed, being stomatal closure the only hindrance for photosynthesis for flooded *Nr* plants, it is arguably likely that these plants are better prepared to resume growth once the stress recedes. Nevertheless, the mutant could be less fit to tolerate long periods of stress if senescence does not timely accompany the photosynthesis decline (Grbić and Bleeker 1995). Namely, the maintenance of green leaves that photosynthesize below the compensation point in *Nr* could result in costly sink organs importing sugar and nutrients (Fig. S3E,F; Grbić and Bleeker 1995).

In conclusion, our data indicate that ethylene perception through the NR/ETR3 receptor has deleterious effects on the photosynthetic capacity maintenance of leaves from flooded tomato plants. Indeed, flooding-induced ethylene would impair both light and dark photosynthesis reactions by hastening the processes that lead to the dismantling of

the photosynthetic apparatus. Moreover, we show that NR-mediated ethylene signalling cascade would halt leaf expansion limiting in this way light capture and carbon uptake in plants under flooding conditions (Fig. 8).

Acknowledgements – We are very grateful to Prof. Piero Picciarelli and Dr Lorenzo Guglielminetti for giving us the opportunity to carry out experiments at the Plant Physiology Lab of the Department of Agriculture, Food and Environment of the University of Pisa. We also thank Dr Tommaso Michele Moles for providing assistance during laboratory work and Mr. Elvis Firulete for his invaluable support. This work was supported by grant A008/16 from SGCyT-UNNE (Universidad Nacional del Nordeste).

Author contributions

L.F.D.P., F.M., M.L.V., and A.S. designed the experiments; L.F.D.P. performed photosynthesis, chlorophyll fluorescence measurements and leaf pigment analysis; F.M. performed soluble protein content quantification, total protease activity analysis, gene expression analysis and biomass allocation experiment; J.P.M. performed RcbL quantification; A.S. and L.F.D.P. analysed the data; L.F.D.P., F.M. and M.L.V. wrote the manuscript; C.A.B. critically revised and corrected the manuscript proof.

Data availability statements

The data that support the findings of this study are available from the corresponding author upon reasonable request.

References

Abeles F, Morgan P, Saltveit M Jr. (2012) Ethylene in plant biology 2nd Edn. Academic Press, San Diego

Ahsan N, Lee DG, Lee SH, Kang KY, Bahk JD, Choi MS, Lee IJ, Renaut J, Lee BH (2007) A comparative proteomic analysis of tomato leaves in response to waterlogging stress. Physiol Plant 131: 555-570

Arbona V, López-Climent, MF, Pérez-Clemente RM, Gómez-Cadenas A (2009) Maintenance of a high photosynthetic performance is linked to flooding tolerance in citrus. Environ Exp Bot 66: 135-142

Ashraf M, Rehman H (1999) Interactive effects of nitrate and long-term waterlogging on growth, water relations, and gaseous exchange properties of maize (*Zea mays* L.). Plant Sci 144: 35-43

Ashraf MA (2012) Waterlogging stress in plants: a review. Afr J Agric Res 7: 1976-1981

Bailey-Serres J, Lee SC, Brinton E (2012) Waterproofing crops: effective flooding survival strategies. Plant Physiol 160: 1698-1709

Battelli R, Lombardi L, Rogers HJ, Picciarelli P, Lorenzi R, Ceccarelli N (2011) Changes in ultrastructure, protease and caspase-like activities during flower senescence in *Lilium longiflorum*. Plant Sci 180: 716-725

Bernacchi CJ, Singsaas EL, Pimentel C, Portis AR Jr, Long SP (2001) Improved temperature response functions for models of Rubisco-limited photosynthesis. Plant Cell Environ 24: 253-259

Bertin N, Gary C (1998) Short and long term fluctuations of the leaf mass per area of tomato plants - Implications for growth models. Ann Bot 82: 71-81

Bhatt RM, Upreti KK, Divya MH, Bhat S, Pavithra CB, Sadashiva AT (2015) Interspecific grafting to enhance physiological resilience to flooding stress in tomato (*Solanum lycopersicum* L.). Sci Hortic 182: 8-17

Bradford KJ (1983) Effects of soil flooding on leaf gas exchange of tomato plants. Plant Physiol 73: 475-479

Caser M, Angiolillo FD, Chitarra W, Lovisolo C, Ruffoni B, Pistelli L, Pistelli L, Scariot V (2016) Water deficit regimes trigger changes in valuable physiological and phytochemical parameters in *Helichrysum petiolare* Hilliard and B.L. Burtt. Ind Crops Prod 83: 680-692

Centritto M, Loreto F, Chartzoulakis K (2003) The use of low (CO_2) to estimate diffusional and non-diffusional limitations of photosynthetic capacity of salt-stressed olive saplings. Plant Cell Environ 26: 585-594

Ceusters J, Van de Poel B (2018) Ethylene exerts species-specific and age-dependent control of photosynthesis. Plant Physiol 176: 2601-2612

Chen Y, Cothren JT, Chen DH, Ibrahim AMH, Lombardini L (2015). Ethylene-inhibiting compound 1-MCP delays leaf senescence in cotton plants under abiotic stress conditions. J Integr Agric 14: 1321-1331

Chen Z, Gallie DR (2015) Ethylene Regulates Energy-Dependent Non-Photochemical Quenching in Arabidopsis through Repression of the Xanthophyll Cycle. PLoS ONE 10

Ciardi JA, Tieman DM, Lund ST, Jones JB, Stall RE, Klee HJ (2000) Response to *Xanthomonas campestris* pv. *vesicatoria* in tomato involves regulation of ethylene receptor gene expression. Plant Physiol 123: 81-92

Dall'Osto L, Caffarri S, Bassi R (2005) A mechanism of nonphotochemical energy dissipation, independent from PsbS, revealed by a conformational change in the antenna protein CP26. Plant Cell 17: 1217-1232

Das K, Roychoudhury A (2014) Reactive oxygen species (ROS) and response of antioxidants as ROS-scavengers during environmental stress in plants. Front Environ Sci 2

Dawood T, Yang X, Visser EJW, Te Beek TAH, Kensche PR, Cristescu SM, Lee S, Floková K, Nguyen D, Mariani C, Rieu I (2016). A co-opted hormonal cascade activates dormant adventitious root primordia upon flooding in *Solanum dulcamara*. Plant Physiol 170: 2351-2364

Demmig-Adams B, Adams WW (2006) Photoprotection in an ecological context: the remarkable complexity of thermal energy dissipation. New Phytol 172: 11-21

Djanaguiraman M, Prasad PVV, Al-Khatib K (2011) Ethylene perception inhibitor 1-MCP decreases oxidative damage of leaves through enhanced antioxidant defense

mechanisms in soybean plants grown under high temperature stress. Environ Exp Bot 71: 215-223

Drake R, John I, Farrell A, Cooper W, Schuch W, Grierson D (1996) Isolation and analysis of cDNAs encoding tomato cysteine proteases expressed during leaf senescence. Plant Mol Biol 30: 755-767

Ella ES, Kawano N, Yamauchi Y, Tanaka K, Ismail A (2003) Blocking ethylene perception enhances flooding tolerance in rice seedlings. Funct Plant Biol 30: 813-819

Else MA, Janowiak F, Atkinson CJ, Jackson MB (2009) Root signals and stomatal closure in relation to photosynthesis, chlorophyll a fluorescence and adventitious rooting of flooded tomato plants. Ann Bot 103: 313-323

Ezin V, De La Pena R, Ahanchede A (2010) Flooding tolerance of tomato genotypes during vegetative and reproductive stages. Braz J Plant Physiol 22: 131-142

Farquhar GD, Von Caemmerer S, Berry JA (1980) A biochemical model of photosynthetic CO_2 assimilation in leaves of C3 species. Planta 149: 78-90

Flexas J, Díaz-Espejo A, Berry JA, Cifre J, Galmés J, Kaldenhoff R, Medrano H, Ribas-Carbó M (2007) Analysis of leakage in IRGA's leaf chambers of open gas exchange systems: Quantification and its effects in photosynthesis parameterization. J Exp Bot 58: 1533-1543

Fukao T, Xu K, Ronald PC, Bailey-Serres J (2006) A variable cluster of ethylene response factor-like genes regulates metabolic and developmental acclimation responses to submergence in rice. Plant Cell 18: 2021-2034

Gepstein S, Glick BR (2013) Strategies to ameliorate abiotic stress-induced plant senescence. Plant Mol Biol 82: 623-633

Gratão PL, Monteiro CC, Rossi ML, Martinelli AP, Peres LEP, Medici LO, Lea PJ, Azevedo RA (2009) Differential ultrastructural changes in tomato hormonal mutants exposed to cadmium. Environ Exp Bot 67: 387-394

Grbić V, Bleecker AB (1995) Ethylene regulates the timing of leaf senescence in Arabidopsis. Plant J 8: 595-602

Grichko VP, Glick BR. 2001. Flooding tolerance of transgenic tomato plants expressing the bacterial enzyme ACC deaminase controlled by the 35S, rolD or PRB-1b promoter. Plant Physiol Biochem 39: 19-25

Hattori Y, Nagai K, Furukawa S, Song XJ, Kawano R, Sakakibara H, Wu J, Matsumoto T, Yoshimura A, Kitano H, Matsuoka M, Mori H, Ashikari M (2009). The ethylene response factors SNORKEL1 and SNORKEL2 allow rice to adapt to deep water. Nature 460: 1026-1030

Herrera A (2013) Responses to flooding of plant water relations and leaf gas exchange in tropical tolerant trees of a black-water wetland. Front Plant Sci 4: 1-13

Herrera A, Tezara W, Marín O, Rengifo E (2008) Stomatal and non-stomatal limitations of photosynthesis in trees of a tropical seasonally flooded forest. Physiol Plant 134: 41-48

Horchani F, Aloui A, Brouquisse R, Aschi-Smiti S (2008) Physiological responses of tomato plants (*Solanum lycopersicum*) as affected by root hypoxia. J Agron Crop Sci 194: 297-303

Jackson MB (2002) Long-distance signalling from roots to shoots assessed: The flooding story. J Exp Bot 53: 175-181

Jullien A, Allirand JM, Mathieu A, Andrieu B, Ney B (2009) Variations in leaf mass per area according to N nutrition, plant age, and leaf position reflect ontogenetic plasticity in winter oilseed rape (*Brassica napus* L.). Field Crops Res 114: 188-197

Kawase M (1974) Role of ethylene in induction of flooding damage in sunflower. Physiol Plant 31: 29-38

Kawase M (1981) Effect of ethylene on aerenchyma development. Am J Bot 68: 651-658

Khan NA, Mir MR, Nazar R, Singh S (2008) The application of ethephon (an ethylene releaser) increases growth, photosynthesis and nitrogen accumulation in mustard (*Brassica juncea* L.) under high nitrogen levels. Plant Biol 10: 534-538

Khanna-Chopra R (2012) Leaf senescence and abiotic stresses share reactive oxygen species-mediated chloroplast degradation. Protoplasma 249: 469-481

Kläring HP, Zude M (2009) Sensing of tomato plant response to hypoxia in the root environment. Sci Hort 122: 17-25

Kozlowski TT (1984) Plant responses to flooding of soil. BioScience 34: 162-167

Kundzewicz ZW, Mata LJ, Arnell NW, Doll P, Kabat P, Jimenez B, Miller KA, Oki T, Sen, Z., Shiklomanov IA (2007) Freshwater resources and their management. Climate change 2007: impacts, adaptation and vulnerability. In: Parry ML, Canziani, OF, Palutikof JP, Van der Linden PJ, Hanson CE, (eds) Contribution of working group II to

the fourth assessment report of the intergovernmental panel on climate change. Cambridge University Press, Cambridge, pp 173–210

Lanahan MB, Yen HC, Giovannoni JJ, Klee HJ (1994) The Never ripe mutation blocks ethylene perception in tomato. Plant Cell 6: 521-530

Lichtenthaler HK (1987) Chlorophylls and carotenoids: pigments of photosynthetic biomembranes. Method Enzymol 148: 350-382

Lincoln JE, Cordes S, Read E, Fischer RL (1987) Regulation of gene expression by ethylene during *Lycopersicon esculentum* (tomato) fruit development. Proc Natl Acad Sci USA 84: 2793-2797

Mariotti L, Fambrini M, Scartazza A, Picciarelli P, Pugliesi C (2018) Characterization of lingering hope, a new brachytic mutant in sunflower (*Helianthus annuus* L.) with altered salicylic acid metabolism. J Plant Physiol 231: 402-414

Masood A, Iqbal N, Khan NA (2012) Role of ethylene in alleviation of cadmium-induced photosynthetic capacity inhibition by sulphur in mustard. Plant Cell Environ 35: 524-533

Mielke MS, Schaffer B (2010) Leaf gas exchange, chlorophyll fluorescence and pigment indexes of *Eugenia uniflora* L. in response to changes in light intensity and soil flooding. Tree Physiol 30: 45-55

Mignolli F, Mariotti L, Lombardi L, Vidoz ML, Ceccarelli N, Picciarelli P (2012) Tomato fruit development in the auxin-resistant *dgt* mutant is induced by pollination but not by auxin treatment. J Plant Physiol 169: 1165-1172

Mignolli F, Todaro JS, Vidoz ML (2020) Internal aeration and respiration of submerged tomato hypocotyls are enhanced by ethylene-mediated aerenchyma formation and hypertrophy. Physiol Plant 169: 49-63

Mishra SK, Patro L, Mohapatra PK, Biswal B (2008) Response of senescing rice leaves to flooding stress. Photosynthetica 46: 315-371

Moles MT, Pompeiano A, Huarancca T, Scartazza A, Guglielminetti L (2016) The efficient physiological strategy of a tomato landrace in response to short-term salinity stress. Plant Physiol Biochem 109: 262-272

Monteiro CC, Carvalho RF, Gratão PL, Carvalho G, Tezotto T, Medici LO, Peres LEP, Azevedo RA (2011) Biochemical responses of the ethylene-insensitive *Never ripe* tomato mutant subjected to cadmium and sodium stresses. Environ Exp Bot 71: 306-320

Montgomery J, Goldman S, Deikman J, Margossian L, Fischer RL (1993) Identification of an ethylene-responsive region in the promoter of a fruit ripening gene. Proc Natl Acad Sci USA 90: 5939-5943

Morgan PW, Drew MC (1997) Ethylene and plant responses to stress. Physiol Plant 100: 620-630

Mutava RN, Prince SJ, Syed NH, Song L, Valliyodan B, Chen W, Nguyen HT (2015) Understanding abiotic stress tolerance mechanisms in soybean: a comparative evaluation of soybean response to drought and flooding stress. Plant Physiol Biochem 86: 109-120

Najeeb U, Bange MP, Tan DK, Atwell BJ (2015) Consequences of waterlogging in cotton and opportunities for mitigation of yield losses. AoB Plants 7: 1-17

Parry MAJ, Andralojc PJ, Khan S, Lea PJ, Keys AJ (2002) Rubisco activity: Effects of drought stress. Ann Bot 89: 833-839

Parry MAJ, Keys AJ, Madgwick PJ, Carmo-Silva, AE, Andralojc PJ (2008) Rubisco regulation: A role for inhibitors. J Exp Bot 59:1569-1580

Pedersen O, Perata P, Voesenek LA (2017) Flooding and low oxygen responses in plants. Funct Plant Biol 44: 3-6

Peng HP, Chan CS, Shih MC, Yang SF (2001). Signaling events in the hypoxic induction of alcohol dehydrogenase gene in Arabidopsis. Plant Physiol 126: 742-749

Peuke AD, Gessler A, Trumbore S, Windt CW, Homan N, Gerkema E, Van As H (2015) Phloem flow and sugar transport in *Ricinus communis* L. is inhibited under anoxic conditions of shoot or roots. Plant Cell Environ 38: 433-447

Pezeshki SR (2001) Wetland plant responses to soil flooding. Environ Exp Bot 46: 299-312

Pierik R, Tholen D, Poorter H, Visser EJ, Voesenek LA (2006) The Janus face of ethylene: growth inhibition and stimulation. Trends Plant Sci 11: 176-183

Pirrello J, Prasad BCN, Zhang W, Chen K, Mila I, Zouine M, Latché A, Pech JC, Ohme-Takagi M, Regad F, Bouzayen M (2012) Functional analysis and binding affinity of tomato ethylene response factors provide insight on the molecular bases of plant differential responses to ethylene. BMC Plant Biol 12: 190

Pompeiano A, Huarancca Reyes T, Moles TM, Guglielminetti L, Scartazza A (2019) Photosynthetic and growth responses of *Arundo donax* L. plantlets under different oxygen deficiency stresses and reoxygenation. Front Plant Sci 10: 408

Poór P, Kovács J, Borbély P, Takács Z, Szepesi Á, Tari I (2015) Salt stress-induced production of reactive oxygen- and nitrogen species and cell death in the ethylene receptor mutant *Never ripe* and wild type tomato roots. Plant Physiol Biochem 97: 313-322

Quirino BF, Noh YS, Himelblau E, Amasino RM (2000) Molecular aspects of leaf senescence. Trends Plant Sci 5: 278-82

Sade N, Del Mar Rubio-Wilhelmi M, Umnajkitikorn K, Blumwald E (2018) Stress-induced senescence and plant tolerance to abiotic stress. J Exp Bot 69: 845-853

Sasidharan R, Bailey-Serres J, Ashikari M, Atwell BJ, Colmer TD, Fagerstedt K, Fukao T, Geigenberger P, Hebelstrup KH, Hill RD, Holdsworth MJ, Ismail AM, Licausi F, Mustroph A, Nakazono M, Pedersen O, Perata P, Sauter M, Shih M-C, Sorrell BK, Striker GG, van Dongen JT, Whelan J, Xiao S, Visser EJW, Voesenek LACJ (2017). Community recommendations on terminology and procedures used in flooding and low oxygen stress research. New Phytol 214: 1403-1407

Sasidharan R, Voesenek LA (2015) Ethylene-mediated acclimations to flooding stress. Plant Physiol 169: 3-12

Scartazza A, Di Baccio D, Pierangelo B, Gavrichkova O, Matteucci G (2016) Investigating the European beech (*Fagus sylvatica* L.) leaf characteristics along the vertical canopy profile: leaf structure, photosynthetic capacity, light energy dissipation and photoprotection mechanisms. Tree Physiol 36: 1060-1076

Smethurst CF, Shabala S (2003) Screening methods for waterlogging tolerance in lucerne: comparative analysis of waterlogging effects on chlorophyll fluorescence, photosynthesis, biomass and chlorophyll content. Funct Plant Biol 30: 335-343

Sone C, Ito O, Sakagami JI (2012) Characterizing submergence survival strategy in rice via chlorophyll fluorescence. J Agron Crop Sci 198: 152-160

Stearns JC, Glick BR (2003) Transgenic plants with altered ethylene biosynthesis or perception. Biotechnol Adv 21: 193-210

Striker GG (2012) Flooding stress on plants: anatomical, morphological and physiological responses. In: Mworia JK, (ed). Botany. Rijeka, Croatia: InTech, 226.

Tholen D, Pons TL, Voesenek LACJ, Poorter H (2007) Ethylene insensitivity results in down-regulation of Rubisco expression and photosynthetic capacity in tobacco. Plant Physiol 144: 1305-1315

Tholen D, Voesenek LACJ, Poorter H (2004) Ethylene insensitivity does not increase leaf area or relative growth rate in Arabidopsis, *Nicotiana tabacum*, and *Petunia* x *hybrida*. Plant Physiol 134: 1803-1812

Tournier B, Sanchez-Ballesta MT, Jones B, Pesquet E, Regad F, Latché A, Pech JC, Bouzayen M (2003) New members of the tomato ERF family show specific expression pattern and diverse DNA-binding capacity to the GCC box element. FEBS Lett 550: 149-154

Van Oosten JJ, Besford RT (1994) Sugar feeding mimics effect of acclimation to high CO_2- rapid down regulation of RuBisCO small subunit transcripts but not of the large subunit transcripts. J Plant Physiol 143: 306-312

van Veen H, Mustroph A, Barding GA, Vergeer-van Eijk M, Welschen-Evertman RAM, Pedersen O, Visser EJW, Larive CK, Pierik R, Bailey-Serres J., Voesenek LACJ, Sasidharan R (2013). Two Rumex species from contrasting hydrological niches regulate flooding tolerance through distinct mechanisms. Plant Cell 25: 4691-4707

Vidoz ML, Loreti E, Mensuali A, Alpi A and Perata P (2010) Hormonal interplay during adventitious root formation in flooded tomato plants. Plant J 63: 551-562

Vidoz ML, Mignolli F, Aispuru HT, Mroginski, LA (2016) Rapid formation of adventitious roots and partial ethylene sensitivity result in faster adaptation to flooding in the *aerial roots* (*aer*) mutant of tomato. Sci Hort 201: 130-139

Voesenek LA, Sasidharan R (2013) Ethylene - and oxygen signalling - drive plant survival during flooding. Plant Biol 15: 426-435

Weraduwage SM, Chen J, Anozie FC, Morales A, Weise SE, Sharkey TD (2015) The relationship between leaf area growth and biomass accumulation in *Arabidopsis thaliana*. Front Plant Sci 6

Westbeek MHM, Pons TL, Cambridge ML, Atkin OK (1999) Analysis of differences in photosynthetic nitrogen use efficiency of alpine and lowland *Poa* species. Oecologia 120: 19-26

Wi SJ, Jang SJ, Park KY (2010) Inhibition of biphasic ethylene production enhances tolerance to abiotic stress by reducing the accumulation of reactive oxygen species in *Nicotiana tabacum*. Mol Cells 30: 37-49

Yamauchi T, Tanaka A, Mori H, Takamure I, Kato K, Nakazono M (2016). Ethylene-dependent aerenchyma formation in adventitious roots is regulated differently in rice and maize. Plant Cell Environ 39: 2145-2157

Yamauchi T, Watanabe K, Fukazawa A, Mori H, Abe F, Kawaguchi K, Oyanagi A, Nakazono M (2014) Ethylene and reactive oxygen species are involved in root aerenchyma formation and adaptation of wheat seedlings to oxygen-deficient conditions. J Exp Bot 65: 261-273Yeung E, van Veen H, Vashisht D, Paiva ALS, Hummel M, Rankenberg T, Steffens B, Steffen-Heins A, Sauter M, de Vries M, Schuurinkg RC, Bazinh J, Bailey-Serres J, Voesenek LACJ, Sasidharan R (2018) A stress recovery signaling network for enhanced flooding tolerance in *Arabidopsis thaliana*. Proc Natl Acad Sci U S A 115: E6085-E6094

Yordanova RY, Popova LP (2007) Flooding-induced changes in photosynthesis and oxidative status in maize plants. Acta Physiol Plant 29: 535-541

Yordanova RY, Uzunova AN, Popova LP (2005) Effects of short-term soil flooding on stomata behaviour and leaf gas exchange in barley plants. Biol Plantarum 49: 317-319

Figure legends

Fig. 1. Relative expression levels of ethylene-responsive genes *MSRA* (A) and *SlERF-A2* (B) in leaves of Pearson (PRS) and *Never ripe* (*Nr*) in control and flooded plants after 2 days from the onset of the stress. Each bar represents the mean ± SD (n = 3). For each gene, expression of PRS control was set to one. Different letters indicate

statistically significant differences (one-way ANOVA with Tukey's HSD multiple comparison test, $P < 0.05$).

Fig. 2. Leaf pigment changes in Pearson (PRS) and *Never ripe* (*Nr*) plants under control and flooding conditions. Photographs of the 3rd fully expanded leaves from PRS and *Nr* plants, bars indicate 1 cm (A). Green colour intensity expressed as SPAD units at 2, 4 and 6 days of flooding in PRS and *Nr* (B). Values are the mean ± SEM (n = 5). Different letters indicate statistical differences within each time point (one-way ANOVA with Tukey's HSD multiple comparison test, $P < 0.05$). Content of chlorophyll *a*, Chl *a* (C); chlorophyll *b*, Chl *b* (D); total carotenoids, Car (E); and total carotenoids to chlorophyll ratio, Car/Chl (*a*+*b*) (F). Analyses were performed using the 3rd fully expanded leaf after 6 days of flooding. Values are the mean ± SEM (n = 5). In graphs (C, D, E), different letters indicate statistically significant differences within each time point ($P < 0.05$ by the Kruskal–Wallis test). In graph (F), different letters indicate statistical differences according to one-way ANOVA with Tukey's HSD multiple comparison test ($P < 0.05$).

Fig. 3. Chlorophyll fluorescence parameters in control and flooded Pearson (PRS) and *Never ripe* (*Nr*) plants. Maximum quantum efficiency of PSII (F_v/F_m) (A), Actual quantum yield (Φ_{PSII}) (B), Non-Photochemical Quenching (NPQ) (C). Values represent the mean ± SEM (n = 8). Measurements were carried out on the terminal leaflet of the 3rd fully expanded leaf at 2, 4 and 6 days after the start of flooding. For graphs A and C, different letters indicate statistical difference within each time point according to

one-way ANOVA with Tukey's HSD multiple comparison test ($P < 0.05$). For graph B, different letters indicate statistically significant differences within each time point ($P < 0.05$ by the Kruskal–Wallis test).

Fig. 4. Leaf gas exchange analysis in Pearson (PRS) and *Never ripe* (*Nr*) plants exposed to control and flooding conditions. Net carbon assimilation rate, A (A); stomatal conductance, g_s (B); transpiration rate, E (C); intercellular CO_2 concentration, C_i (D). All measurements were performed in the terminal leaflet of the 3rd fully expanded leaf after 2, 4 and 6 days from the onset of flooding. Each bar represents the mean ± SEM (n = 8). For graphs A and C, different letters indicate statistical differences within each time point according to one-way ANOVA with Tukey's HSD multiple comparison test ($P < 0.05$). For graphs B and D, different letters indicate statistically significant differences within each time point ($P < 0.05$ by the Kruskal–Wallis test).

Fig. 5. Photosynthesis efficiency parameters of Pearson (PRS) and *Never ripe* (*Nr*) leaves from control and flooded plants. Intrinsic Water Use Efficiency (WUEi) expressed as the result of A to g_s ratio at 2, 4, and 6 days from the beginning of the stress (A). Each bar represents the mean ± SEM (n = 8). Different letters indicate statistical differences within each time point according to one-way ANOVA with Tukey's HSD multiple comparison test ($P < 0.05$). Carboxylation efficiency (B). Each point represents net CO_2 assimilation rate (A) and intercellular CO_2 concentration (C_i) values obtained at each level of ambient CO_2 concentrations (C_a) (50 to 400 µmol

mol^{-1}) in leaves after 6 days of flooding. Vertical bars represent *A* SEM (n = 3) and horizontal bars represent C_i SEM (n = 3). Each line represents the linear regression. Maximum rate of Rubisco carboxylation (Vc_{max}) (C) at the 6th day of flooding. Each bar represents the mean ± SEM (n = 8) and different letters indicate statistical differences (one-way ANOVA with Tukey's HSD multiple comparison test, $P < 0.05$).

Fig. 6. Rubisco gene expression. Relative transcript abundance of Rubisco large, *rbcL* (A) and small subunit, *rbcS* (B) genes. Each point represents means ± SD (n = 3) and the value of PRS control plants at time 0 was set to one. Samples of the 3rd fully expanded leaves were analysed. Different letters indicate statistical differences within each time point according to one-way ANOVA with Tukey's HSD multiple comparison test ($P < 0.05$).

Fig. 7. Leaf protein content and expression of protease genes. Relative abundance of RbcL protein (A). Leaf proteins were electrophoretically separated. 56kD bands, corresponding to RbcL, were quantified and RbcL abundance of control PRS plants was set to one. Each bar represents means ± SEM (n = 3). Total soluble proteins (B), total protease activity (C) and transcription levels of cysteine protease genes (D, E, F) in 3rd fully expanded leaves of Pearson (PRS) and *Never ripe* (*Nr)* plants after 6 days from the start of control and flooding treatments. All analyses were performed on the 3rd fully expanded leaves after 6 days from the beginning of flooding. Values of total soluble proteins and total protease activity are means ± SEM (n = 5). Values of cysteine

protease genes transcripts are means ± SD (n = 3) and the value of PRS control plants for each gene was set as one. Different letters indicate statistical differences according to one-way ANOVA with Tukey's HSD multiple comparison test ($P < 0.05$).

Fig. 8. Photosynthesis of flooded tomato plants with impaired ethylene sensitivity. Stomatal closure in response to flooding decreases CO_2 availability for carboxylation (stomatal-limitation) and causes downregulation of Rubisco *rcbL* and *rcbS* genes transcription. Ethylene, which is produced in response to flooding, is perceived by the Never Ripe/ETR3 receptor which causes the initiation of a premature senescence process. Leaf area reduction and pigment loss are believed to impair both light capture and exceeding energy dissipation mechanisms, affecting PSII efficiency. In addition, the upregulation of cysteine protease (CYP) genes causes leaf protein dismantling and the reduction of Rubisco protein content, possibly reducing its carboxylation efficiency (non-stomatal limitation).

Table 1. Growth parameters of control and flooded Pearson (PRS) and *Never ripe* (*Nr)* plants after 6 days from the start of flooding stress. Data are the mean ± SD; number of replicates between parenthesis. Means with a common letter are not significantly different ($P > 0.05$ non-parametric Kruskal-Wallis test).

Supporting Information

Fig. S1. Leaf pigment content in the 4th fully expanded leaf of Pearson (PRS) and *Never ripe* (*Nr*) in control and flooded plants. Different letters indicate statistical differences (one-way ANOVA with Tukey's multiple comparison test, $P < 0.05$).

Fig. S2. Analysis of chlorophyll fluorescence and leaf gas exchange of the 4th fully expanded leaf in Pearson (PRS) and *Never ripe* (*Nr*) plants exposed to control and flooding conditions. In graphs a-d, different letters indicate statistical differences within each time point (one-way ANOVA with Tukey's HSD multiple comparison test, $P < 0.05$). In graphs (e and f), different letters indicate statistical differences according to Kruskal-Wallis test, $P < 0.05$).

Fig. S3. Sucrose (Suc), glucose (Glc) and fructose (Fru) content in 3rd and 4th leaves of Pearson (PRS) and *Never ripe* (*Nr*) plants after 6 days of flooding. Different letters indicate statistical differences (one-way ANOVA with Tukey's HSD multiple comparison test, $P < 0.05$).

Fig. S4. Schematic representation of flooding (partial submersion) experiment set-up (a). In section (b) an example of a 28 week-old tomato plant used in the experiment is shown. Fully expanded leaf positions are labelled with ordinal numbers.

Table S1. List of gene accessions and primer sequences.

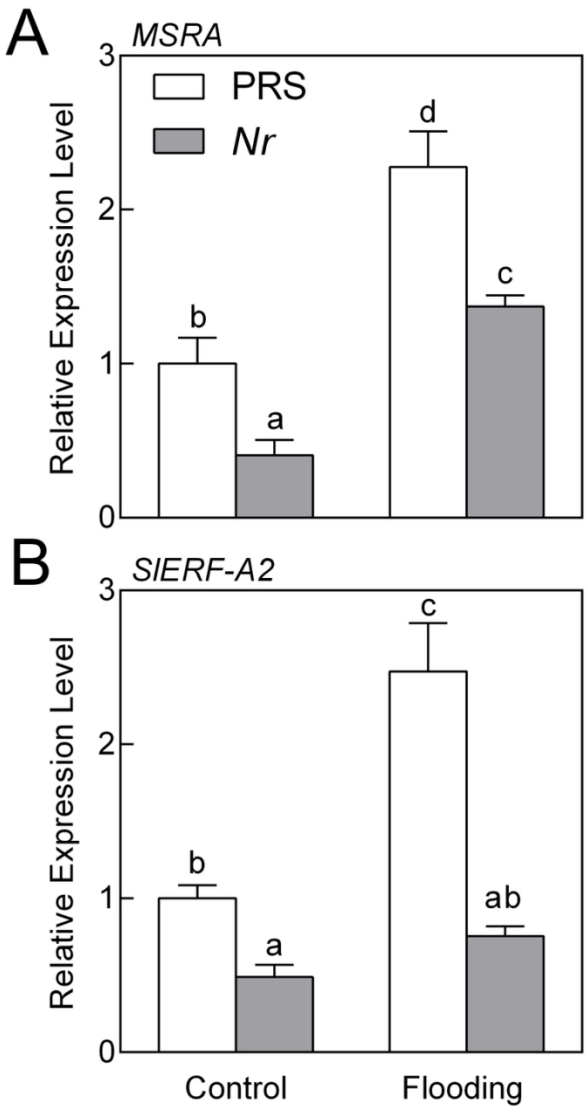

Fig. 1

80x131mm (300 x 300 DPI)

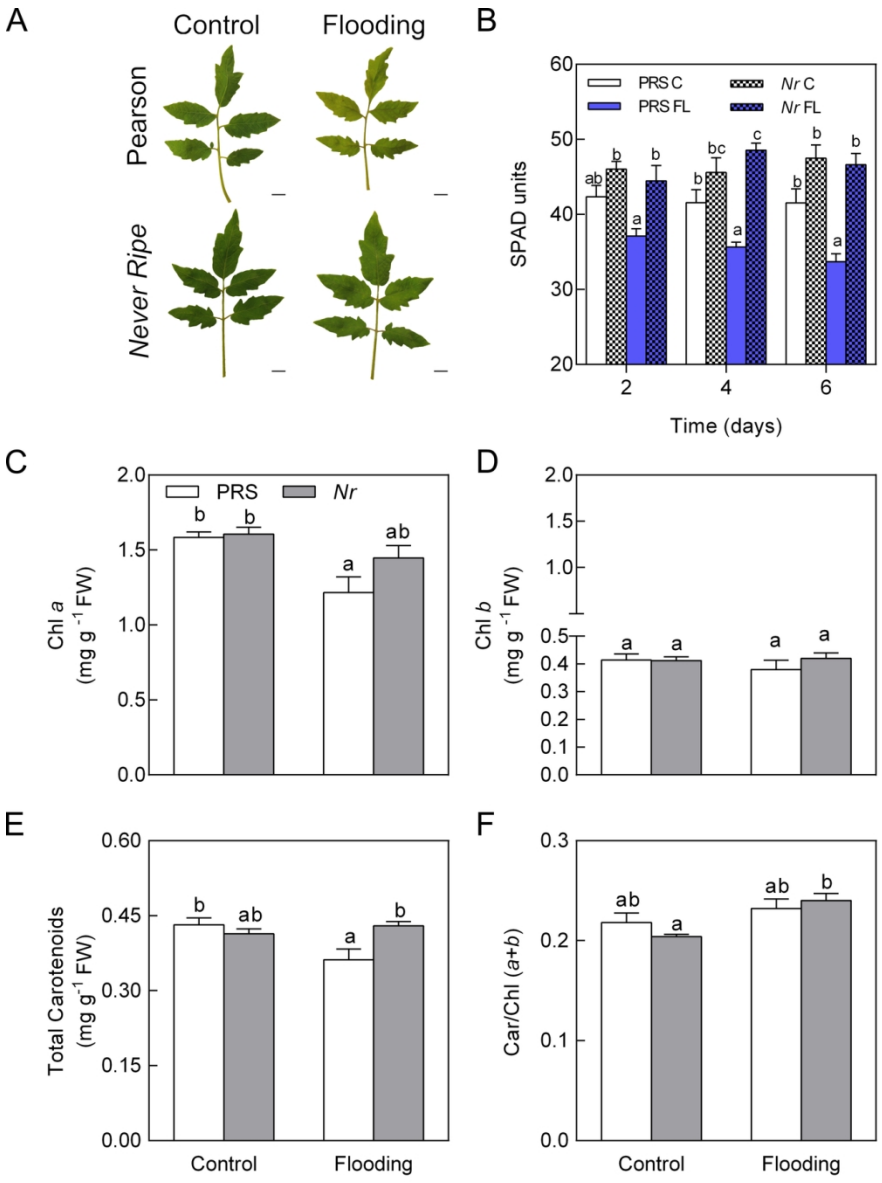

Fig. 2

124x156mm (300 x 300 DPI)

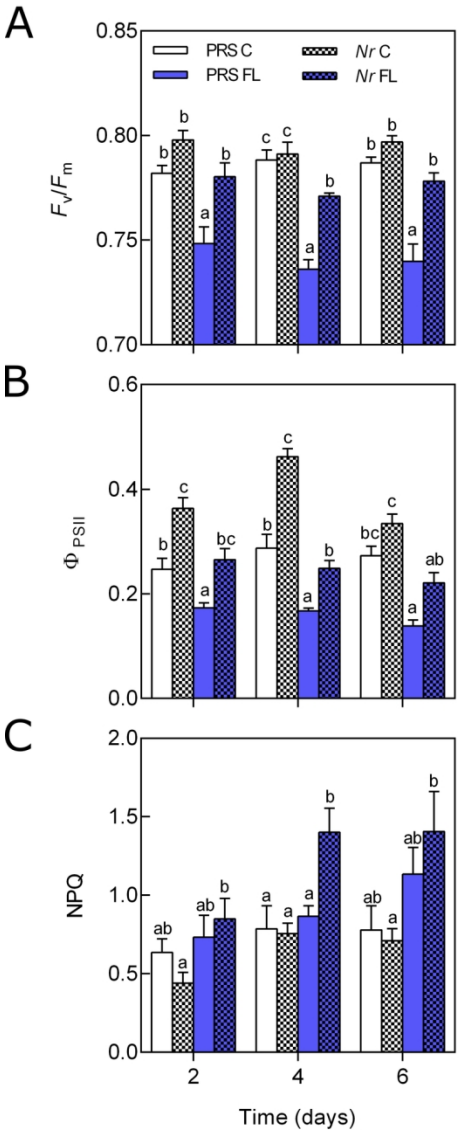

Fig. 3

80x177mm (300 x 300 DPI)

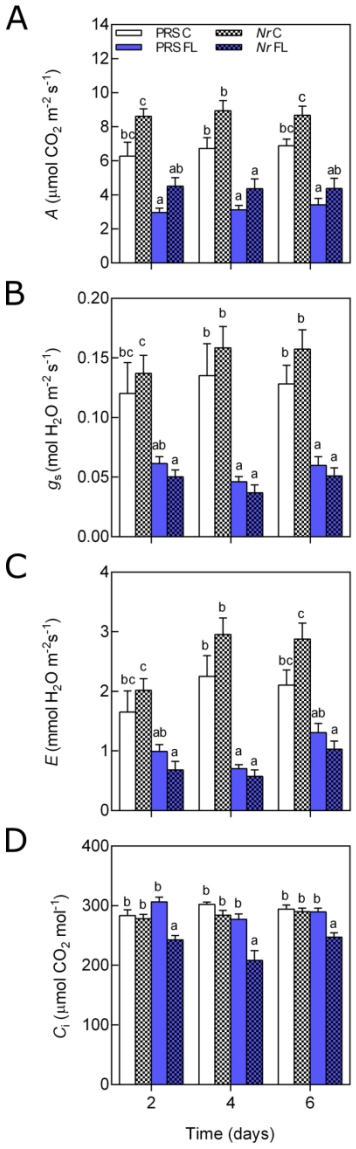

Fig. 4

80x230mm (300 x 300 DPI)

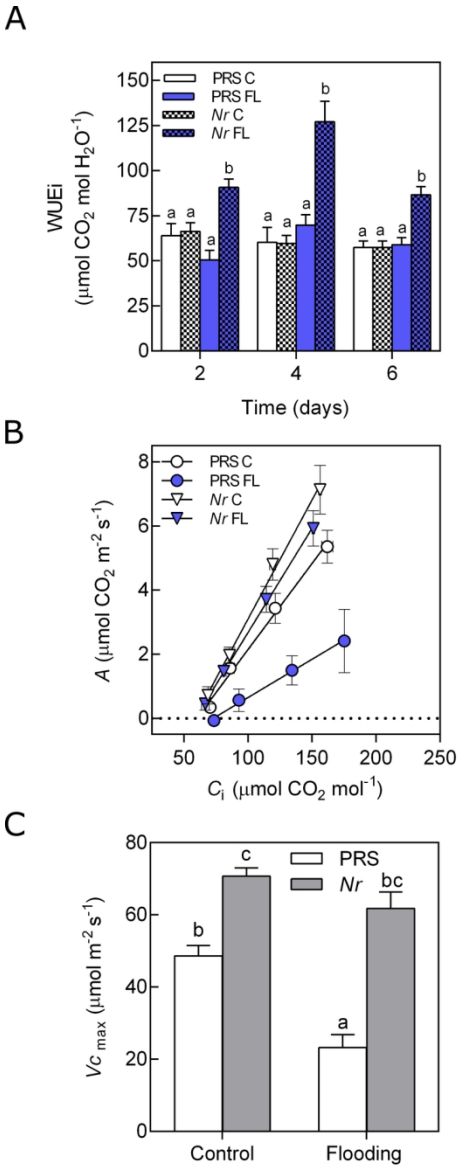

Fig. 5

79x183mm (300 x 300 DPI)

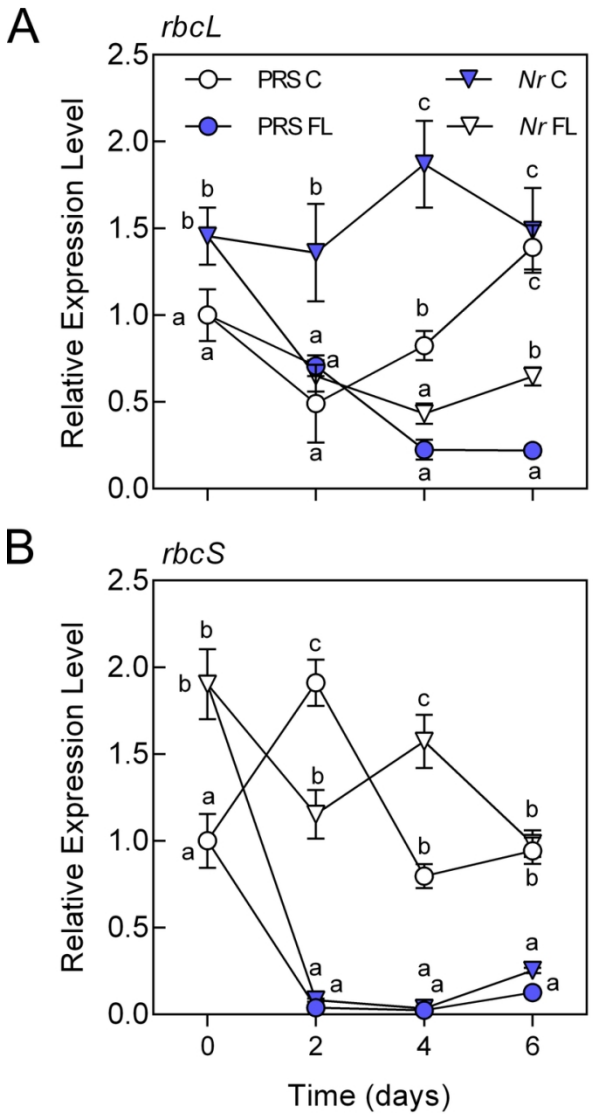

Fig. 6

80x139mm (300 x 300 DPI)

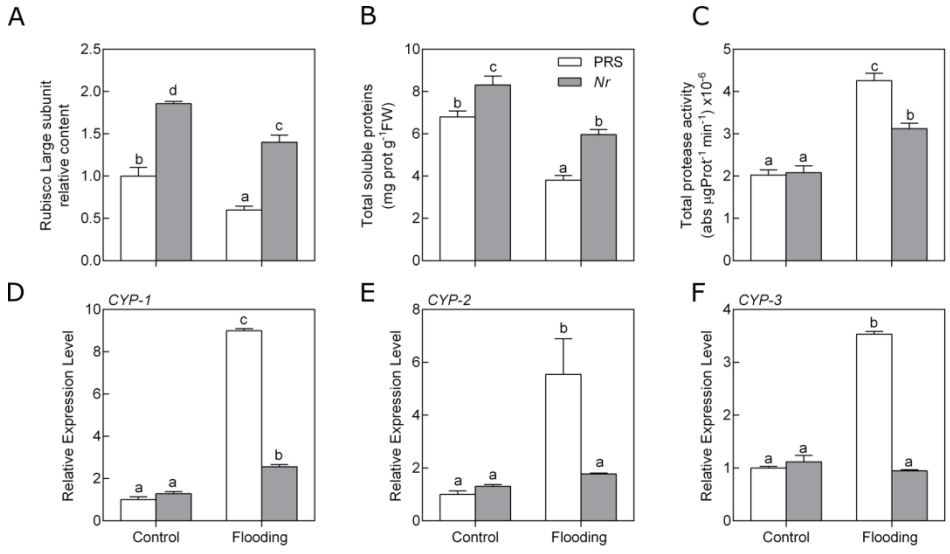

Fig. 7

165x94mm (300 x 300 DPI)

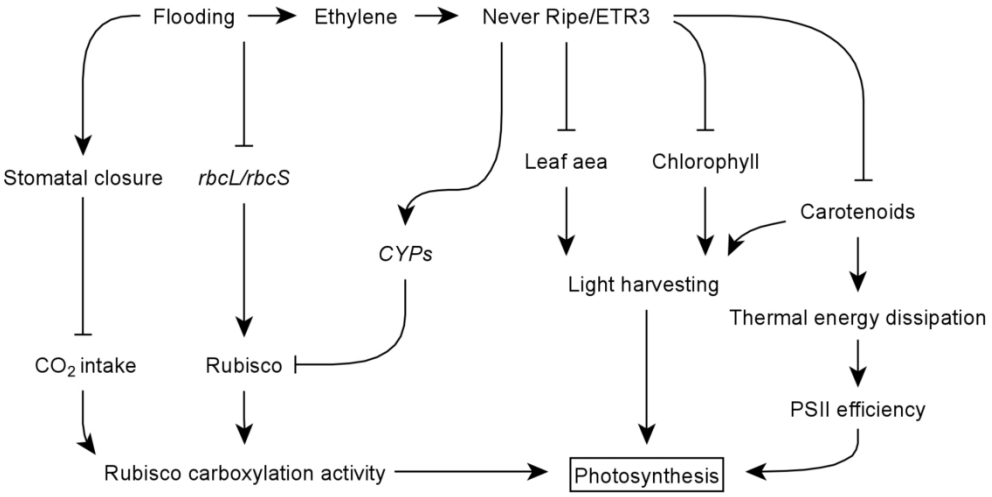

Fig. 8

179x92mm (300 x 300 DPI)

Parameter	Pearson		*Never ripe*	
	Control	Flooding	Control	Flooding
Total biomass (g)	2.57±0.29 (8) b	1.30±0.30 (8) a	2.59 ±0.43 (8) b	1.71±0.19 (8) a
Leaf area (cm^2)	424.2±34.4 (8) c	162.0±92.7 (8) a	382.4±62.5 (8) bc	324.5±30.6 (8) b
LMF (%)	60.1±1.8 (8) b	48.8±3.8 (8) a	61.3±7.6 (8) b	55.6±1.7 (8) a
SMF (%)	27.8±1.7 (8) a	44.1±3.1 (8) b	29.4±2.2 (8) a	39.0±1.7 (8) b
RMF (%)	12.0±1.4 (8) b	3.2±0.7 (8) a	12.0±1.0 (8) b	3.2±1.3 (8) a
SLA ($mm^2\ mg^{-1}$)	27.7±2.7 (8) a	25.1±10.5 (8) a	24.7±5.6 (8) a	34.4±3.3 (8) b